NASA TECHNICAL MEMORANDUM

NASA TM X-2406

NASA TM X-2406

EMPIRICAL EXPRESSIONS FOR ESTIMATING LENGTH AND WEIGHT OF AXIAL-FLOW COMPONENTS OF VTOL POWERPLANTS

by David A. Sagerser, Seymour Lieblein, and Richard P. Krebs

Lewis Research Center
Cleveland, Ohio 44135

NATIONAL AERONAUTICS AND SPACE ADMINISTRATION • WASHINGTON, D. C. • DECEMBER 1971

1. Report No.	2. Government Accession No.	3. Recipient's Catalog No.
NASA TM X-2406		

4. Title and Subtitle	5. Report Date
EMPIRICAL EXPRESSIONS FOR ESTIMATING LENGTH AND WEIGHT OF AXIAL-FLOW COMPONENTS OF VTOL POWERPLANTS	December 1971
	6. Performing Organization Code

7. Author(s)	8. Performing Organization Report No.
David A. Sagerser, Seymour Lieblein, and Richard P. Krebs	E-6191
	10. Work Unit No. 721-03

9. Performing Organization Name and Address	11. Contract or Grant No.
Lewis Research Center National Aeronautics and Space Administration Cleveland, Ohio 44135	
	13. Type of Report and Period Covered
12. Sponsoring Agency Name and Address	Technical Memorandum
National Aeronautics and Space Administration Washington, D.C. 20546	14. Sponsoring Agency Code

15. Supplementary Notes

16. Abstract

Simplified equations are presented for estimating the length and weight of major powerplant components of VTOL aircraft. The equations were developed from correlations of lift and cruise engine data. Components involved include fan, fan duct, compressor, combustor, turbine, structure, and accessories. Comparisons of actual and calculated total engine weights are included for several representative engines.

17. Key Words (Suggested by Author(s))		18. Distribution Statement
V/STOL aircraft	Fan	Unclassified - unlimited
Aircraft engines	Compressor	
Weight (mass)	Combustor	
Length	Turbine	

19. Security Classif. (of this report)	20. Security Classif. (of this page)	21. No. of Pages	22. Price*
Unclassified	Unclassified	39	$3.00

* For sale by the National Technical Information Service, Springfield, Virginia 22151

EMPIRICAL EXPRESSIONS FOR ESTIMATING LENGTH AND WEIGHT OF AXIAL-FLOW COMPONENTS OF VTOL POWERPLANTS

by David A. Sagerser, Seymour Lieblein, and Richard P. Krebs

Lewis Research Center

SUMMARY

Expressions for estimating the length and weight of axial flow components are presented in this report. These expressions were developed from correlated lift and cruise engine data with the aid of simplified component models. Components involved include fan, fan duct, compressor, combustor, turbine, structure, and accessories. The expressions were developed primarily for use in parametric analyses of powerplants suitable for VTOL transport aircraft.

Because of differences in reported details as well as in design approaches, considerable variability was noted in the component data. However, when comparisons were made between estimated and actual total engine weight for several representative engines, good agreement was found for nearly all cases considered.

Discussions of the use and limitations of the developed expressions are also included in the report.

INTRODUCTION

Parametric studies of propulsion systems for VTOL transport aircraft are being conducted at the Lewis Research Center to evaluate the comparative design and performance characteristics of candidate systems. Propulsion systems for VTOL aircraft involve turbojet, turbofan, compressed air generator, and exhaust gas generator powerplants. These powerplants are described in reference 1 and representative examples are shown in figure 1.

Cycle performance studies alone may not be sufficient for analysis of VTOL powerplants. Studies have shown that propulsion system weight can amount to as much as 30 percent of the gross weight of a VTOL transport (e.g., refs. 2 to 4). Likewise, the volume of the propulsion system represents a significant fraction of the complete

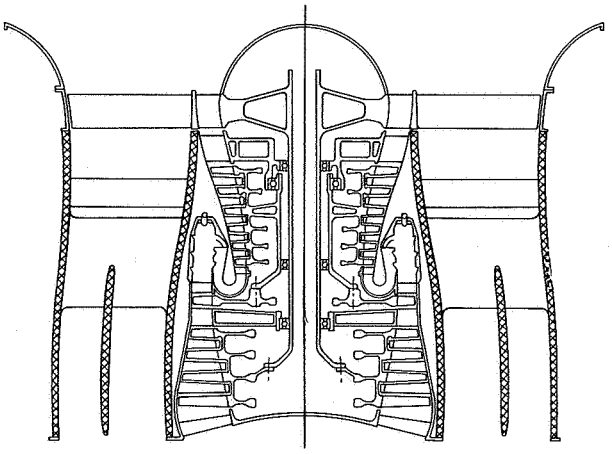

Turbofan

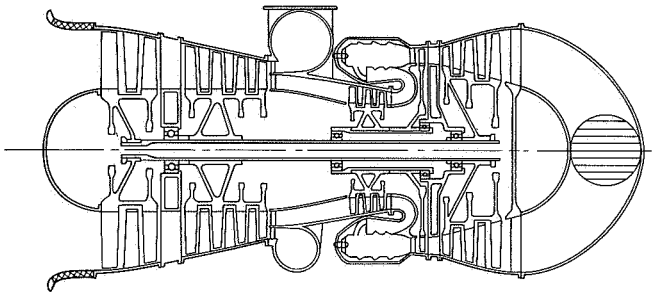

Compressed air generator (used with remote lift fan)

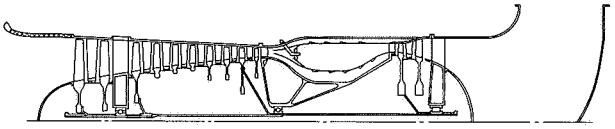

Exhaust gas generator (used with remote lift fan)

Figure 1. - Examples of VTOL powerplant concepts.

airplane. It is therefore desirable to know the size (dimensions) and weight of propulsion system components along with the thermodynamic performance in order for more significant comparisons to be made. A step toward obtaining these propulsion system characteristics is to estimate the uninstalled powerplant length and weight.

Accurate weight and length characteristics are generally available when a detailed mechanical design is made for a specific powerplant configuration. However, such a procedure would prove to be too costly and time consuming if a large number of configurations are to be parametrically examined. Simplified estimating methods are therefore needed that will consistently estimate length and weight trends with reasonable ac-

curacy. These methods should be sufficiently detailed to reflect the type of powerplant, thrust level, component arrangement and design, and advances in component technology.

Methods have been developed, as described in references 5 to 7, to estimate gas turbine engine weights, but they were not specifically applicable for the types of powerplants considered for the VTOL applications described in reference 1. Gerend and Roundhill's method (ref. 5) will not reflect changes in component arrangement or design techniques. Steven's method (ref. 6) for estimating rotor characteristics was considered too detailed for parametric studies, while for other components the assumptions seemed too restrictive to apply to widely differing design approaches. Merriman's method (ref. 7) gives simplified relations for scaling components of similar design, but it requires additional judgment in choosing coefficients to reflect variations in design approaches. The previous methods, however, gave direction and insight to this effort.

This report describes the correlations developed for length and weight estimates of the major components that might be involved in powerplants for VTOL propulsion systems. Components involved include fan, fan duct, compressor, combustor, turbine, structure, and accessories. Remote fans, which would be part of the propulsion systems utilizing either compressed air or exhaust gas generators, were not included in this effort. Also not included were installation requirements, that is, inlets, nacelles, etc., as they are dependent on the airplane configuration.

The derived relations were based on correlations of information from a number of advanced technology gas turbine engines (both lift and cruise). When used in conjunction with specified cycle conditions and component arrangements, these relations allowed for the estimation of length and weight for VTOL powerplants representative of the data from which the correlations were obtained. These correlations may give insight into the effects of changes in design variables and component improvements on overall powerplant length and weight. They may also serve as a useful reference for other studies. It should be emphasized, however, that the resulting length and weight estimates apply to the powerplants only and not to installed propulsion systems.

APPROACH AND DATA SOURCES

Correlations of component characteristics are not likely to result in exact expressions because there is no single design method that is used universally. Variations from one designer to another as well as changes in materials and design techniques with time account for significant differences between components meeting equal aerodynamic performance requirements. Component correlations, then, will be approximations at best, with consistency of trend as their principal goal.

In recognition of the impossibility of deducing exact expressions, the data were correlated in terms of only first-order variables. In particular, it was desired to include

the effect of component gross size (i. e., outer or mean diameter) plus any other major physical or aerothermodynamic variables as required that could be related to the cycle parameters. In some cases simplified analytical models were used to determine the form and significant variables for the estimating equations. The available data were then used to determine the correlating coefficients for the equations.

The correlations were accomplished by graphical means rather than by more sophisticated statistical methods. This was done because of the limited amount of data and because of the judgment involved in attaching significance to each data point.

The components for which correlations of length were developed are the following: fan, compressor, combustor, and turbine. Components for which correlations of weight were developed are the following: fan, fan duct, compressor, combustor, turbine, accessories, and structure. Total engine length, excluding the inlet and nozzle, was found by adding the lengths of the appropriate components. The lengths of transition ducts and structural struts additive to the engine length, which may be necessary in particular engine designs, were not considered here. Similarly, total uninstalled powerplant weight is found by addition of the weights of the appropriate components.

The data used in the correlations were obtained from a number of documents on the characteristics of three types of advanced engines: lift, cruise, and lift-cruise. These engines were in various stages of development: preliminary design, demonstrator, or production. Most of the data involved engines in the preliminary design stage. The number and development stage of engines used in the correlations are given in table I according to component. The type of engine used for a particular correlation is indicated in the data figures.

The data were differentiated both as to type and to development status so that differences in data groups could be accounted for in the correlation process. It was assumed, however, that the relations among the major parameters in each estimating equation would be consistent for all engines. For example, differences were found between lift engine data and cruise engine data in most of the component weights. The form of the equations was determined using all of the data, while the differences in engine type were factored out by using different values of the proportionality constant.

Implicit in the proportionality constant and form of each relation developed is a range of values for the variables for which the relation is applicable. For example, the weight of a component will not vary with diameter at very small diameters in the same way that it will vary at larger diameters. In this example, minimum gage thicknesses as well as changes in fabrication techniques are encountered at the very small diameters. Similarly, there are limits on the other variables. The exact limits on each variable, however, are difficult to define in general. The limits for one variable may be a function of the values of the other variables in the relation. As some indication of the range of applicability, table II gives the range of variables for the data used in developing the relations. The correlating variables and their relations are discussed in later sections.

TABLE I. - NUMBER AND STAGE OF DEVELOPMENT

OF DATA USED IN CORRELATIONS

Component	Correlation	Number of data points			
		Total	Production	Demonstrator	Preliminary design
Fan	Rotor aspect ratio	20	3	5	12
	Weight	17	1	2	14
Compressor	Length	37	9	8	20
	Tip speed	27	7	10	10
	Weight	26	2	4	20
Combustor	Length	19	3	6	10
	Pressure loss	19	8	7	4
	Weight	21	2	5	14
Turbine	Rotor aspect ratio	17	3	4	10
	Stator aspect ratio	13	9	1	3
	Weight	28	2	5	21
Controls and accessories	Weight	10	0	5	5
Structure	Weight	14	0	4	10

TABLE II. - RANGE OF DATA FOR CORRELATING VARIABLES

Component	Estimated characteristic	Correlating variable	Range for data
Fan	Rotor aspect ratio	Hub-tip diameter ratio	0.28 to 0.50
	Weight	Tip diameter, m (ft)	0.73 to 2.6 (2.4 to 8.5)
		Rotor aspect ratio	2.5 to 7.7
		Number of stages	1 to 2
Compressor	Length	Number of stages	2 to 16
		Inlet hub-tip diameter ratio	0.38 to 0.83
	Tip speed	Number of stages	2 to 16
		Total pressure ratio	1.5 to 15
		Average stage pressure ratio	1.15 to 1.46
	Weight	Mean diameter, m (ft)	0.34 to 0.98 (1.1 to 3.2)
		Number of stages	2 to 14
		Length to inlet mean diameter ratio	0.29 to 1.4
Combustor	Length	Length to height ratio	1.3 to 4.5
		Reference velocity, m/sec (ft/sec)	15 to 27 (49 to 89)
		Airflow, kg/sec (lbm/sec)	22 to 150 (49 to 330)
		Inlet temperature, K (^{o}R)	520 to 830 (940 to 1500)
		Inlet pressure, mn/m^2 (atm)	0.61 to 2.30 (6 to 23)
		Mean diameter, m (ft)	0.40 to 0.79 (1.3 to 2.6)
	Pressure loss	Length to height ratio	1.3 to 4.5
	Weight	Mean diameter, m (ft)	0.40 to 0.91 (1.3 to 3.0)
Turbine	Rotor aspect ratio	Hub-tip diameter ratio	0.52 to 0.89
	Stator aspect ratio	Hub-tip diameter ratio	0.54 to 0.90
	Weight	Mean diameter, m (ft)	0.43 to 1.2 (1.4 to 3.8)
		Number of stages	1 to 6
		Mean speed, m/sec (ft/sec)	120 to 510 (390 to 1700)
Controls and accessories	Weight	Thrust, N (lb)	18 000 to 170 000 (4000 to 38 000)
		SFC, kg/(N-hr) (lbm/lb-hr)	
Structure	Weight	Estimated weight of components, kg (lbm)	100 to 2000 (230 to 4400)

Some difficulty was encountered in collecting the data on a component basis because of differences in engine layouts, structural design, and reported breakdowns and details. Defining a component's length, for instance, was difficult when the component was made integral with a support member. Defining a component's weight was even more difficult because of large variations in the parts that were included in the weight tabulations, as well as variations in the structural loads the component was required to carry. In some cases, when sufficient information was available, adjustments were made to make the data conform to a consistent definition. This was not possible in all cases, which undoubtedly contributed to the scatter in the correlations.

Although both the International System of Units (SI units) and the U. S. Customary Units (i. e., lb, lbm, ft) are used in this report, the original measurements and calculations were made using the U. S. Customary Units.

FAN STAGE

The fan stage model for a turbofan engine as considered here consists of a single rotor, without inlet guide vanes, and a downstream stator as shown in figure 2. However, the data used included some two-stage fans. While some characteristics are ob-

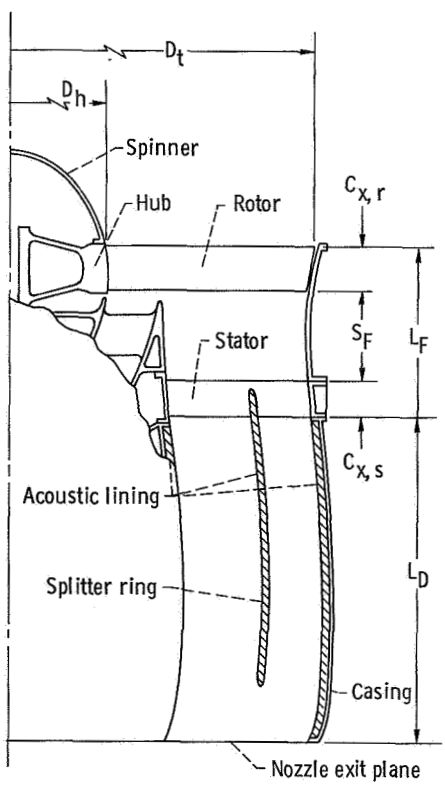

Figure 2. - Fan stage and fan duct model.

viously similar, the fan stage considered here should not be confused with a tip-turbine fan configuration.

Length

The length of the fan stage is expressed by (fig. 2)

$$L_F = C_{x,r} + C_{x,s} + S_F \tag{1}$$

(Definitions of the symbols used in this report may be found in appendix A.) The rotor axial chord $C_{x,r}$ was calculated from the inlet hub and tip diameters (determined, for example, from engine cycle calculations) by

$$C_{x,r} = \frac{(D_t - D_h)_1}{2(AR)_{x,r}} \tag{2}$$

where the fan rotor axial aspect ratio $(AR)_{x,r}$ was defined as the ratio of the inlet blade height to the rotor axial chord at the hub.

No correlation of fan rotor axial aspect ratio with the major fan design parameters could be found from the data. The data were plotted in figure 3 with respect to fan inlet hub-tip diameter ratio. A value of 4.5 appears to be representative of current design practice.

Noise considerations will probably be the chief factor in determining the axial spacing between the rotor and stator for a particular design. The axial spacing between the

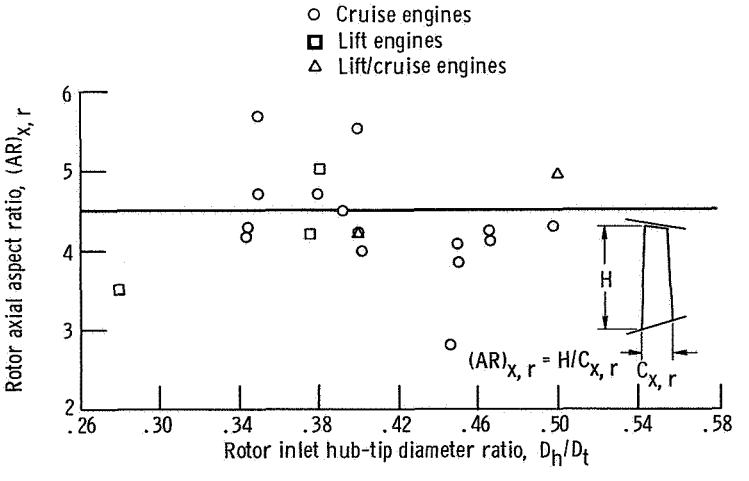

Figure 3. - Fan rotor blade aspect ratio (inlet stage only).

rotor and stator is frequently related to the rotor axial chord length at the blade tip. For simplicity, it was assumed that the rotor axial chord was constant from hub to tip. Equation (1) can then be expressed as

$$L_F = C_{x,r}(1 + a_F) + C_{x,s} \tag{3}$$

where

$$a_F = \left(\frac{S_F}{C_{x,r}}\right)$$

For low-noise designs a minimum value of $a_F = 2$ may be considered representative. However, the design value used depends on the compromise made between noise and fan length.

A similar relation to equation (2) may be used to determine the stator axial chord. The stator aspect ratio can be determined by aerodynamic requirements as well as by noise considerations. In some cases the stator blades also serve as support struts. In such designs, the aspect ratio may be based on mechanical requirements. No general correlation of stator aspect ratio was found.

Weight

The weight of the fan stage as defined herein includes the rotor blades, rotor hub and spinner, stator blades, outer casing, and support struts (which may be integral with the stators). From a simplified theoretical analysis of the fan stage, it was found that the weight equation can be of the form

$$W_F = K_F(D_t)^{3-a} N\left[\frac{(\sigma_t)_r^b}{(\overline{AR}_r)^c}\right] U_t^d \tag{4}$$

where $0 < a, b, c, d < 1$. This equation carries the implication of a relatively consistent relation between stator and rotor blade aspect ratios and solidities. The average rotor aspect ratio $\overline{AR}_r$ used in this equation is defined as the ratio of the average blade height to the average actual blade chord. However, for simplicity, it was assumed that

$$\overline{AR}_r = (AR)_{x,r}$$

When the fan weight data were correlated with equation (4), no dependence on fan tip speed U_t or rotor blade tip solidity $(\sigma_t)_r$ could be found. The relation for the diameter D_t, number of stages N, and rotor aspect ratio was established as

$$W_F = K_F (D_t)^{2.7} \frac{N}{(AR)_{x,r}^{0.5}} \tag{5}$$

where

$$K_F = 135 \qquad (K_F = 12 \text{ for } D_t \text{ in ft, } W_F \text{ in lbm})$$

This correlation is shown in figure 4. No distinction was found between lift engine fan

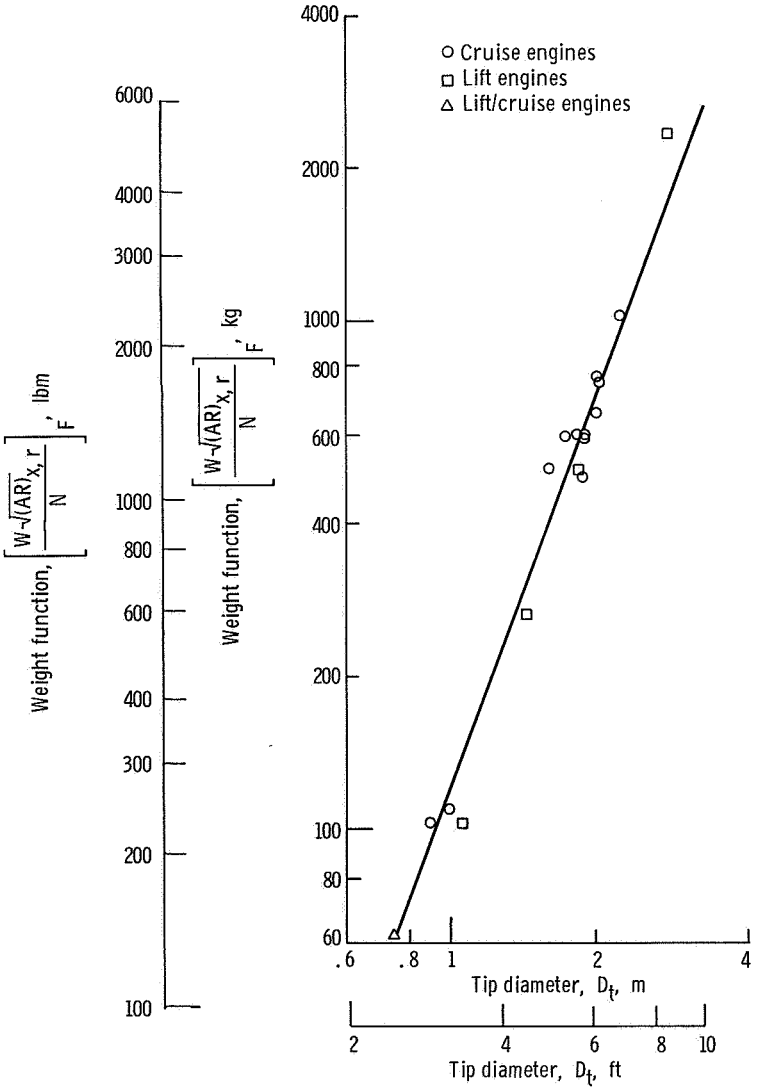

Figure 4. - Fan weight correlation.

weights and cruise engine fan weights.

Although the data did not allow the relation of fan tip speed and solidity to be determined, these parameters surely affect fan weight. For parametric studies where large variations in these parameters may be considered, their effect should be included. Since the data did not show the dependence of fan weight on blade solidity and tip speed, the effect of variations in these parameters are probably somewhat less than the effect of aspect ratio variations. A more complete form of equation (5), then, may be expressed as

$$W_F = K_F(D_t)^{2.7} \frac{N}{(AR)_{x,r}^{0.5}} \left[\frac{\sigma_t}{(\sigma_t)_{Ref}}\right]^{0.3} \left[\frac{U_t}{(U_t)_{Ref}}\right]^{0.3} \tag{6}$$

where the exponents for solidity and tip speed are estimated values. From the data, reference (average) values for solidity $(\sigma_t)_{Ref}$ and tip speed $(U_t)_{Ref}$ were 1.25 and 350 meters per second (1150 ft/sec), respectively.

The fans included in the correlation primarily had solid titanium blades. Significant reductions in fan weight may be possible with hollow blade construction or the use of composite materials. In order to reflect these advanced design techniques, adjustments to the value of K_F may be made in the fan weight estimating equations.

FAN DUCT WEIGHT

Depending on the installation, lift fan engines may require additional length L_D to the bypass duct (outer wall) aft of the fan stator in order to have essentially coplanar core and bypass nozzles (as shown in fig. 2). This duct will also be required to provide for additional acoustic treatment of the fan exhaust. In this section expressions are given for estimating the weight of the duct as well as for the acoustic lining.

The weight of the duct casing W_D was estimated by the simplified expression

$$W_D = \pi \bar{D}_D L_D \left(\frac{W}{A}\right)_D \tag{7}$$

where $\bar{D}_D$ is the average diameter (between inlet and outlet) of the duct casing. The duct weight per unit surface area $(W/A)_D$ represents the product of the average wall thickness $\bar{t}_D$ and the duct material density ρ_D:

$$\left(\frac{W}{A}\right)_D = \rho_D \bar{t}_D$$

Duct wall thicknesses necessary for fabrication, rigidity, and handling are greater than that required for pressure containment for low pressure ratio fans. Therefore, it was assumed the average wall thickness could be taken as a constant. Then, for the same material (constant density) the duct weight per unit surface area will also be constant.

Values of $(W/A)_D$ from engine data varied from 2.4 to 8.3 kilograms per square meter (0.5 to 1.7 lbm/ft^2). A value of 3.5 kilograms per square meter (0.72 lbm/ft^2) was taken to be representative of current design practice for low pressure lift fans. This corresponds to aluminum (ρ = 2770 kg/m^3, 173 lbm/ft^3) with a thickness of 0.13 centimeter (0.05 in.).

Acoustic lining is generally applied to the duct walls as well as to splitter rings concentric to the duct walls as shown in figure 2. The weight of the acoustic lining was estimated similarly to the fan duct casing:

$$W_L = \pi\left[\left(L\bar{D}_h\right)_{\text{inner wall}} + \left(L\bar{D}_t\right)_{\text{outer wall}}\right]\left(\frac{W}{A}\right)_W + \pi\left(\sum_{i=1}^{N_R} L_R D_{R,i}\right)\left(\frac{W}{A}\right)_R \qquad (8)$$

where the number of splitter rings N_R and treated area required depend on the noise suppression desired.

Acoustic lining material is composed of several distinct layers: porous facing, honeycomb core, bonding adhesive, and, in the case of the splitter rings, a solid center sheet. The weight per unit area of the acoustic lining, then, can be expressed as the sum of the weight per unit area of each layer. Values of weight per unit area of the various layers may depend on many factors such as the sound frequency and the duct geometry. However, these factors are complex and difficult to evaluate for preliminary estimates. Thus, for simplicity, a constant representative value of weight per unit area was assumed for each layer.

Values of weight per unit area for acoustic lining (from ref. 8 and unpublished data) varied from 4.4 to 10.7 kilograms per square meter (0.9 to 2.2 lbm/ft^2) for the walls and from 11.2 to 12.7 kilograms per square meter (2.3 to 2.6 lbm/ft^2) for the splitter rings. Since acoustic lining material is in an early development stage, these values are probably conservative. For this reason minimum values from reference 8 were taken to be representative. These values, however, were further reduced to account for an aluminum porous facing layer instead of stainless steel as given in reference 8. This gave for the walls

$$\left(\frac{W}{A}\right)_W = 2.69 \text{ kg/m}^2 \ (0.55 \text{ lbm/ft}^2) \tag{9}$$

and for the splitter rings

$$\left(\frac{W}{A}\right)_R = 8.55 \text{ kg/m}^2 \ (1.75 \text{ lbm/ft}^2) \tag{10}$$

COMPRESSOR

The data for this component were obtained from compressors with both fixed and variable angle stators, constant hub, mean, and tip flow path designs, as well as both disk and drum construction. A diagram of a constant hub compressor model is shown in figure 5.

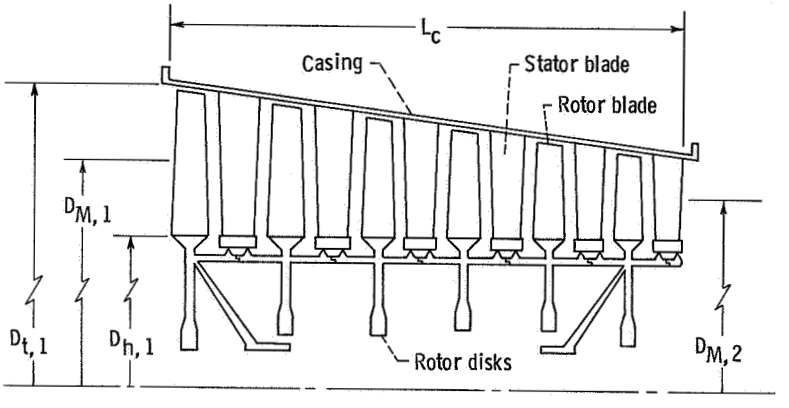

Figure 5. - Compressor model.

Length

In order to estimate compressor length, the ratio of length to inlet mean diameter $L_C/D_{M,1}$ was correlated with the number of stages N and inlet hub-tip diameter ratio $\left(D_h/D_t\right)_1$ to give

$$\frac{L_C}{D_{M,1}} = 0.2 + \left[0.234 - 0.218\left(\frac{D_h}{D_t}\right)_1\right]N \tag{11}$$

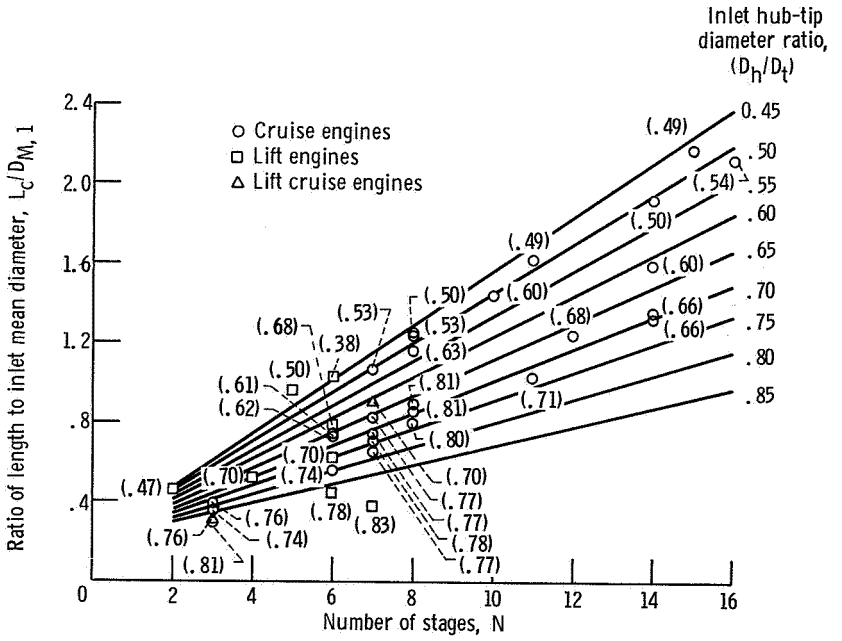

Figure 6. - Correlation of compressor overall length. Values in parenthesis correspond to inlet hub-tip diameter ratios of data points.

Equation (11) is compared with compressor data in figure 6. Some of the compressors had integral structural support struts which added to their actual lengths. In these cases, the length of the support strut was subtracted from the total compressor length so the compressors could be correlated on an equal basis. The effect of flow path design, whether constant hub, mean, or tip, was considered, but neither the data nor simple analysis indicated this to be a significant variable.

The number of stages is related to overall compressor pressure ratio $\left(P_2/P_1\right)_C$ and average stage pressure ratio $\left(\overline{P_2/P_1}\right)_S$ by

$$\left(\frac{\overline{P_2}}{P_1}\right)_S = \left[\left(\frac{P_2}{P_1}\right)_C\right]^{1/N} \tag{12}$$

or

$$N = \frac{\ln\left(\frac{P_2}{P_1}\right)_C}{\ln\left(\frac{\overline{P_2}}{P_1}\right)_S} \tag{13}$$

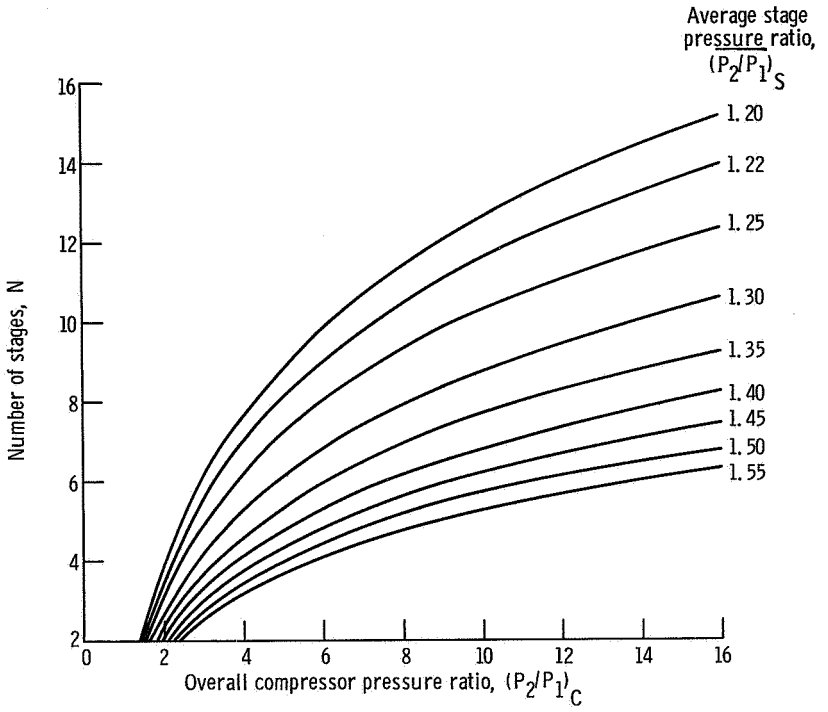

Figure 7. - Relationship of average stage pressure ratio and number of stages to overall compressor pressure ratio.

For convenience, this relation is shown graphically in figure 7. Thus, by specifying the average stage pressure ratio, the number of compressor stages required to develop a desired compressor pressure ratio can be determined. Additional factors must be considered, however, before specifying the average stage pressure ratio.

One such factor, discussed subsequently, is the tip speed. The tip speed will affect the weight and stress of the compressor as well as its drive turbine. The effect of compressor tip speed on noise may also be important.

For constant blade loading, the average stage pressure ratio will be a function of the inlet corrected rotor tip speed and compressor flowpath. Because of reheat effects it will also depend on the overall compressor pressure ratio. A relation between inlet corrected rotor tip speed $(U/\sqrt{\theta})_{C, CMD}$ and average stage pressure ratio was developed from correlations of compressor data and from simplified compressor aerodynamic considerations. This relation is shown in figure 8 for high and moderate loading levels. An analytic curve fit of the relation in figure 8 is given by

$$\left(\frac{U}{\sqrt{\theta}}\right)_{C, CMD} = A\left[\left(\frac{P_2}{P_1}\right)_S + C\left(\frac{P_2}{P_1}\right)_C^{1.8} - B\right] \tag{14}$$

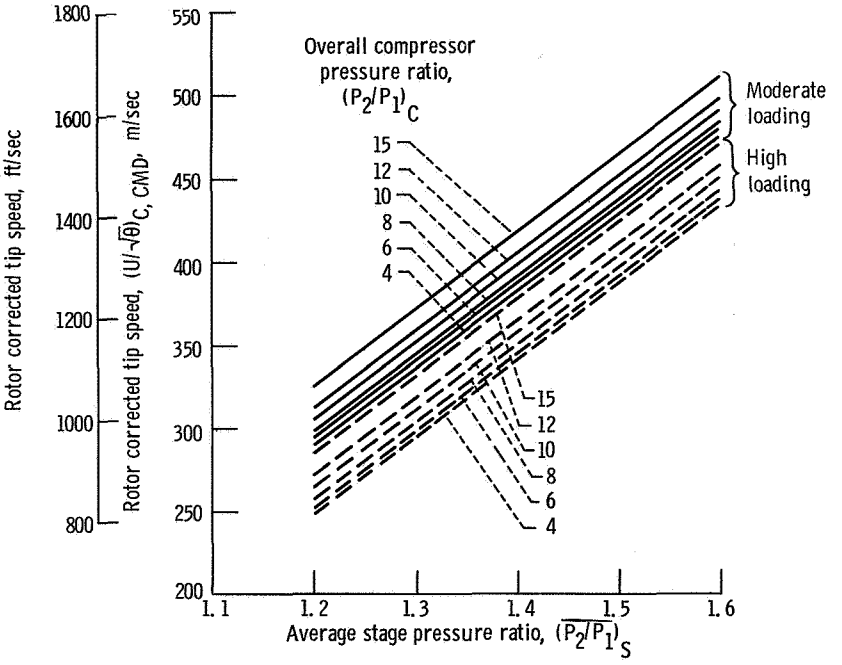

Figure 8. - Relation between compressor tip speed and average stage pressure ratio for constant mean diameter compressors.

where the factor A was taken as 466 (or 1530 for $(U/\sqrt{\theta})_{C, CMD}$ in ft/sec). Factor B is used to reflect blade loading level. Values for high and moderate loading levels were taken as 0.676 and 0.588, respectively. Factor C was taken as 0.654×10^{-3}. This relation was taken to hold for constant mean diameter compressors.

Equation (14) was compared with actual compressor designs as shown in figure 9. The compressor data were plotted by number of stages and corrected rotor tip speed to show comparison with lines of constant average stage pressure ratio from equation (14). It is evident from the figure that equation (14) does not match the data exactly. This may be partially due to the fact that the data were not all from constant mean diameter designs (varied from constant hub to constant tip). The trends, however, do show good agreement and indicate the usefulness of the model.

An adjustment to the average stage pressure ratio was developed to account for the effect of a varying mean diameter design. This adjustment is required because the stage rotor blade speeds (and thus the performance) will be different than for the case of a constant mean diameter compressor with the same inlet tip speed. The average stage pressure ratio for compressors with varying mean diameters $\left(\overline{P_2/P_1}\right)_{S, VMD}$ was deduced as

$$\left(\frac{\overline{P_2}}{P_1}\right)_{S, VMD} = 1 + \left[0.8\left(\frac{D_{M,2}}{D_{m,1}}\right)_C + 0.2\right]\left[\left(\frac{\overline{P_2}}{P_1}\right)_{S, CMD} - 1\right] \tag{15}$$

This relation is shown in figure 10.

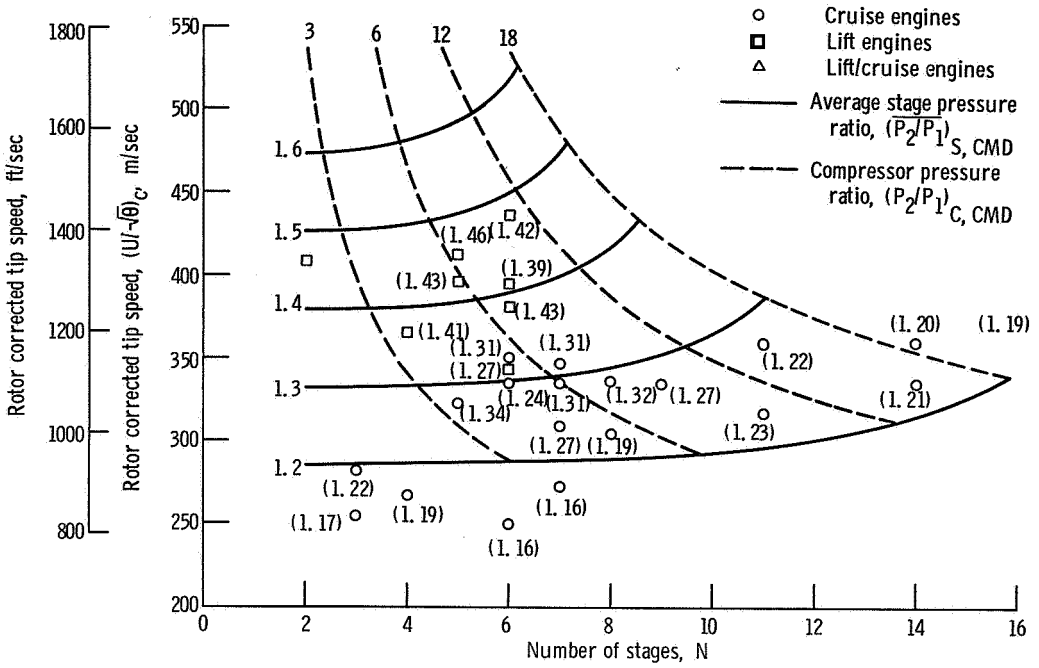

Figure 9. - Compressor tip speed correlation for constant mean diameter, moderate loading model. Values in parenthesis correspond to average stage pressure ratios of data points.

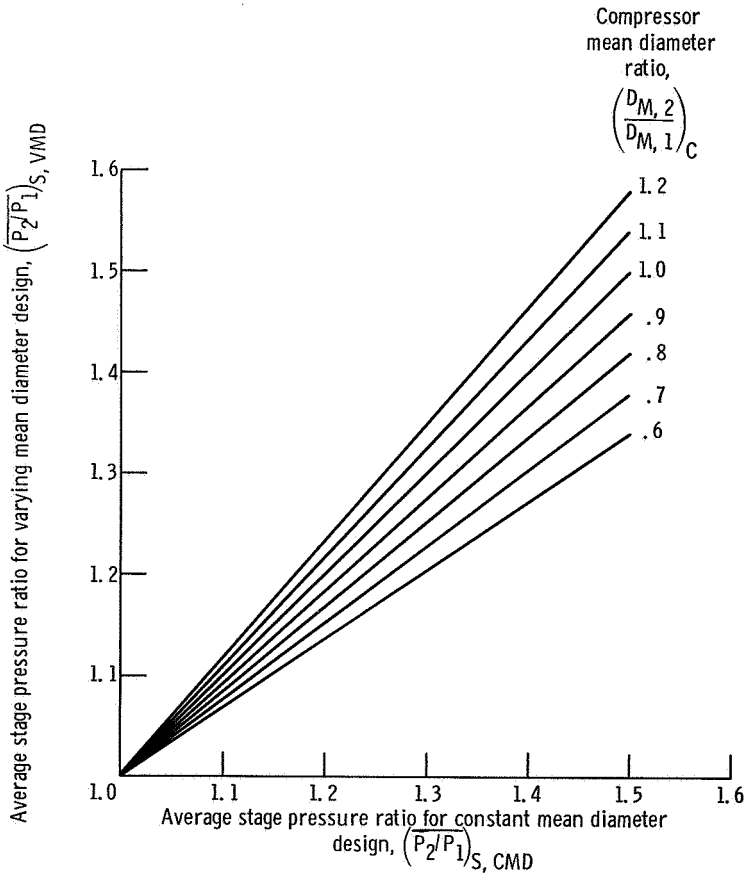

Figure 10. - Effect of mean diameter ratio on compressor average stage pressure ratio.

Equations (14) and (15) were then combined to give a general expression for inlet corrected tip speed:

$$\left(\frac{U}{\sqrt{\theta}}\right)_C = A\left[\frac{\left(\overline{\frac{P_2}{P_1}}\right)_S - 1}{0.8\left(\frac{D_{M,2}}{D_{M,1}}\right) + 0.2} + 1 + C\left(\frac{P_2}{P_1}\right)_C^{1.8} - B\right] \tag{16}$$

where values for the factors A, B, and C are given with equation (14). Equation (16) may be solved for average stage pressure ratio for use with equation (13):

$$\left(\overline{\frac{P_2}{P_1}}\right)_S = 1 + \left[\frac{\left(\frac{U}{\sqrt{\theta}}\right)_C}{A} - C\left(\frac{P_2}{P_1}\right)_C^{1.8} + B - 1\right]\left[0.8\left(\frac{D_{M,2}}{D_{M,1}}\right) + 0.2\right] \tag{17}$$

Weight

The compressor weight is taken to include the rotor blades, disks (or drum), seals, stator blades, and casing. Analysis of a simplified compressor model yielded the following weight equation:

$$W_C = K_C(\overline{D}_M)^{2+a}(N)^{1+b}U_t^c \tag{18}$$

where the average mean diameter $\overline{D}_M$ is defined as

$$\overline{D}_M = \frac{1}{2}(D_{M,1} + D_{M,2})$$

and

$$a < 1, \qquad b < 1, \qquad 0 < c < 1$$

This equation, however, was developed assuming that the length to inlet mean diameter

ratio $L_C/D_{M,1}$ was relatively constant compared to variations in the other variables. As was found in correlating compressor length (fig. 6), $L_C/D_{M,1}$ is dependent on inlet hub-tip diameter ratio. Also, real engine designs vary in the amount of spacing between blade rows which also affects $L_C/D_{M,1}$. Thus, an additional term reflecting variations in $L_C/D_{M,1}$ should be included.

Correlations of compressor data showed equation (18) to be of the following form:

$$W_C = K_C(\overline{D}_M)^{2.2} N^{1.2} \left[1 + \frac{\frac{L_C}{D_{M,1}}}{\left(\frac{L_C}{D_{M,1}}\right)_{Ref}} \right] \tag{19}$$

where $\left(L_C/D_{M.1}\right)_{Ref}$ is a reference length to diameter ratio based on equation (11) assuming $\left(D_h/D_t\right)_1 = 0.7$. Thus, for equation (19)

$$\left(\frac{L_C}{D_{M,1}}\right)_{Ref} = 0.2 + 0.081\,N$$

No effect of compressor tip speed U_t was found from the data.

The weights of lift engine compressors and cruise engine compressors were compared with equation (19) as shown in figure 11. It was evident from the data that lift engine design methods resulted, in this case, in a lighter weight component. This may at least be partially attributed to the more extensive use of titanium. The form of the weight estimating equation was taken the same for both engine types and the difference in levels was accounted for by two values of the proportionality constant in equation (19) where

$K_C = 15.5$ (2.5 for $\overline{D}_M$ in ft) for lift engines

$K_C = 24.2$ (3.9 for $\overline{D}_M$ in ft) for cruise engines

The effect of tip speed may be incorporated into equation (19), as was done in the fan weight equation, in the form

$$W_C = K_C(D_M)^{2.2} N^{1.2} \left[\frac{U_t}{(U_t)_{Ref}}\right]^c \left[1 + \frac{\frac{L_C}{D_{M,1}}}{\left(\frac{L_C}{D_{M,1}}\right)_{Ref}}\right] \tag{20}$$

where c is probably 0.5 or less. The average value of tip speed in the data was 335 meters per second (1100 ft/sec). Then for equation (20)

$$(U_t)_{Ref} = 335 \text{ m/sec } (1100 \text{ ft/sec})$$

A problem arises in estimating the weight of the low spool compressor in a compressed air generator. Low-pressure-ratio low-spool compressors for air generators should be similar to fans in that they have two or three stages, a low inlet hub-tip diameter ratio, and are on a different spool from the gas generator. However, high-pressure-ratio low-spool compressors have many stages and look more like compressors. A suggested solution to this problem is to estimate the weight of the first two

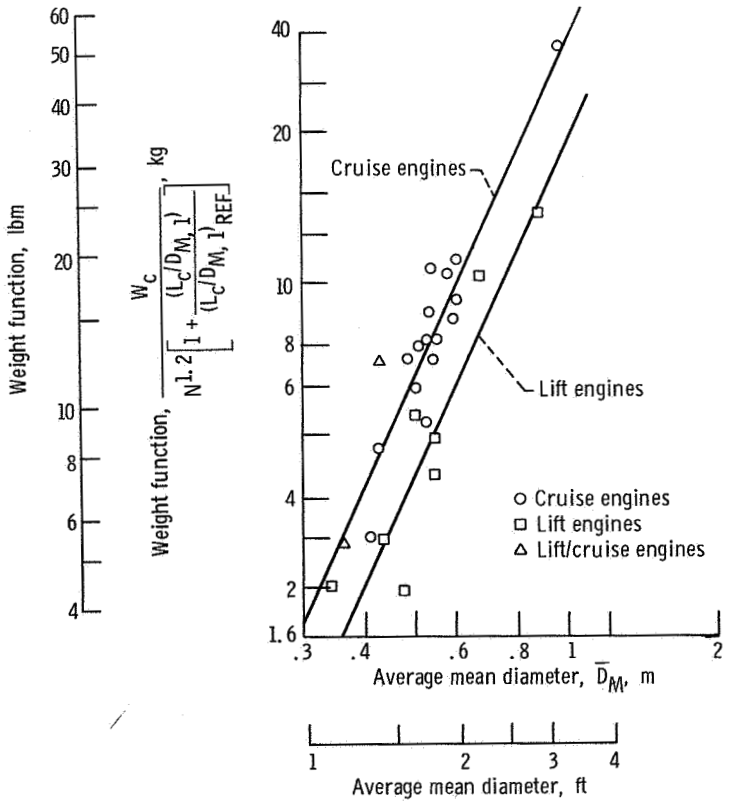

Figure 11. - Compressor weight correlation.

stages using a fan weight equation (eqs. (5) or (6)) and estimate the remaining stages using a compressor weight equation (eqs. (18) or (20)). To avoid unnecessary complexity, the weight of the remaining stages may be estimated by first calculating the weight of the total low spool compressor using a compressor weight equation and then subtracting the calculated weight of the first two stages using the same equation.

COMBUSTOR

The combustors considered were annular axial-flow or reverse-flow designs. Included in this component is the diffuser section. A diagram of an axial-flow combustor model is shown in figure 12.

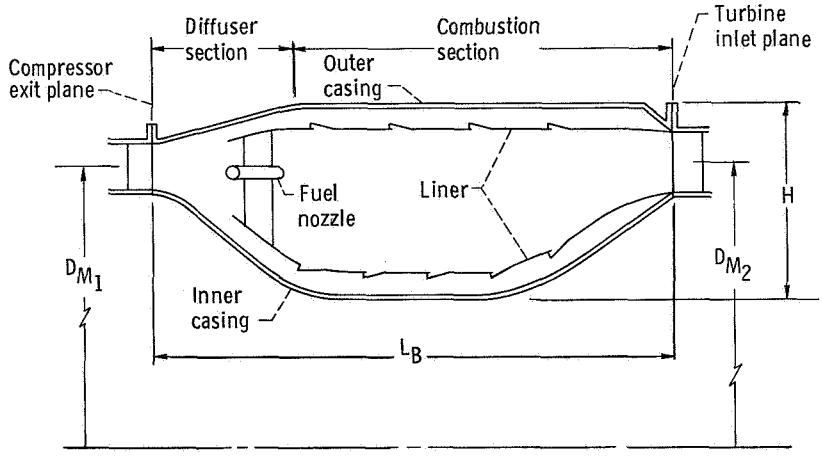

Figure 12. - Combustor model.

Length

In order to estimate the length of a combustor representative of current design practices, data from various engines were correlated based on the assumption that the reference velocity V_{Ref} would be relatively constant for a given class of combustor designs.

The relation expressing the combustor length L_B was developed in terms of the ratio of combustor length to maximum combustor radial height (inner to outer casing) L_B/H as

$$L_B = \left(\frac{L_B}{H}\right)H \tag{21}$$

Then from continuity

$$H = \frac{\dot{w}_a}{\rho_1 \pi \bar{D}_M V_{Ref}} \tag{22}$$

where

$$\bar{D}_M = \frac{1}{2}(D_{M,1} + D_{M,2})$$

Since V_{Ref} is generally small compared to the velocity of sound,

$$\rho_1 = \frac{P_1}{RT_1} \tag{23}$$

Combining equations (21), (22), and (23) gives

$$L_B = \frac{R}{\pi V_{Ref}} \left[\left(\frac{L_B}{H} \right) \left(\frac{\dot{w}_a T_1}{P_1 \bar{D}_M} \right) \right] \tag{24}$$

In applying equation (24) it was assumed that the airflow $\dot{w}_a$, inlet pressure P_1, inlet temperature T_1, and the average mean diameter $\bar{D}_M$, will be known from cycle conditions. However, values for V_{Ref} and L_B/H must be specified. Based on actual combustor data, representative values of V_{Ref} were taken as 18.3 meters per second (60 ft/sec) for cruise engines and 24.4 meters per second (80 ft/sec) for lift engines. Values for L_B/H will be discussed later.

Equation (24) with the assumed values of V_{Ref} was compared with actual combustor data as shown in figure 13. The combustor data were plotted as length against value of the bracket term in equation (24). Since equation (24) is an exact derivative of continuity, the variations in the data from the correlation lines are actually variations in values of V_{Ref}. In order to give a more quantitative indication of this variation, lines corresponding to other than the assumed values of V_{Ref} are also shown in the figure.

The data points shown in figure 13 are all axial-flow designs. Insufficient data were available to correlate reverse-flow combustor lengths. However, the relation developed should be helpful in estimating the lengths of reverse flow combustors as well.

The value of (L_B/H) will in general depend on many factors. Two important considerations are the minimum volume required for burning (heat release rate) and the

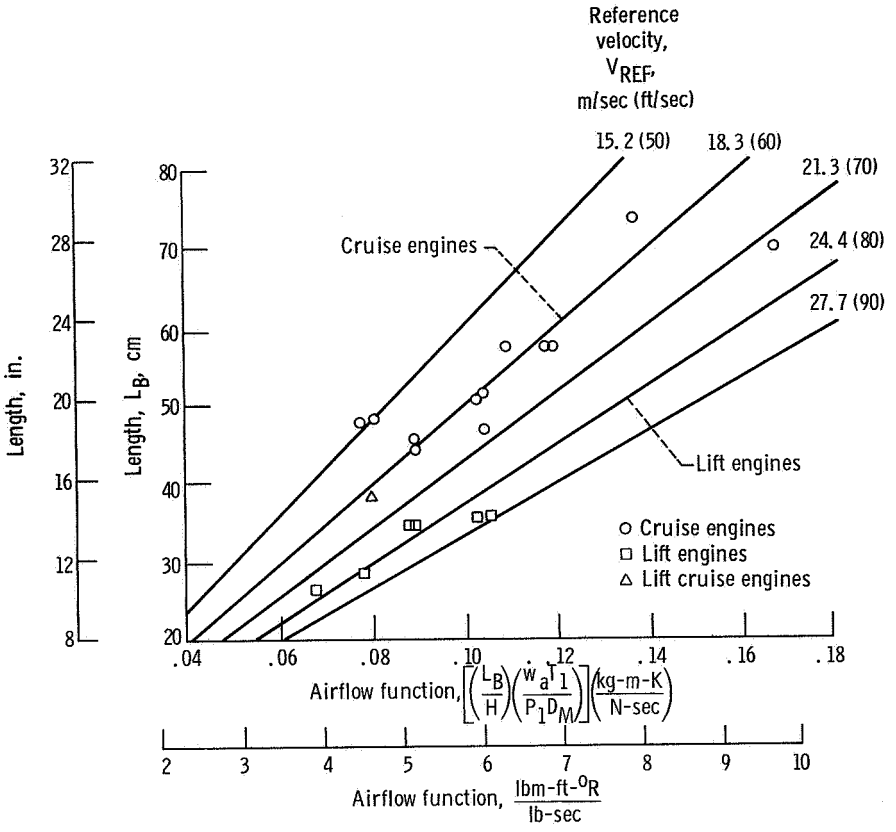

Figure 13. - Axial-flow combustor length and reference velocity correlation (sea level static conditions).

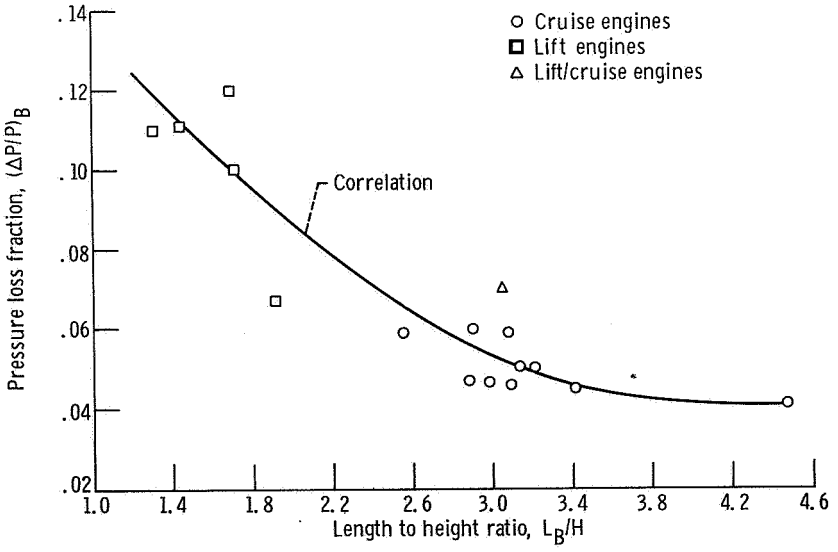

Figure 14. - Correlation for axial combustor pressure loss (sea level static conditions.

allowable total pressure loss for the combustor. A simplified criterion or parameter for determining the minimum volume required for burning was not developed. It was assumed, however, that by keeping the value of (L_B/H) above the minimum found in actual combustor designs, the lower limit on combustor volume may not be exceeded.

A correlation was found between total pressure loss fraction $(\Delta P/P)_B$ and (L_B/H) as shown in figure 14 with high values of (L_B/H) typical of cruise engines and low values typical of lift engines. The trend reflects the effect of higher turbulence required for good mixing in the shorter length combustors. Thus, while shorter more compact combustors are desirable, higher pressure losses can be expected.

Weight

The combustor weight includes the inner and outer casing, liner, and fuel nozzles. Analysis of a simplified combustor model, which assumed the effective thickness of the liner and casings to vary with diameter and gas pressure, gave the following weight equation:

$$W_B = K_B \bar{D}_M^2 L_B P^a \tag{25}$$

where

$$0 < a < 1$$

The relation of length and pressure to combustor weight could not be explicitly determined from the data because of nonuniformities in the reported weight data. Combustor sections may contain varying degrees of structure weight. Also, the weight of bearings, bearing supports, and shafting in the combustor section were often lumped in with the reported weight of the combustor. Finally, some of the lift engine combustors incorporated diluent stators. In these cases the weight of the diluent stators were included in the combustor weight.

Correlation of the combustor weight data was taken as

$$W_B = K_B \bar{D}_M^2 \tag{26}$$

as shown in figure 15. A difference between the weights of cruise engine combustors

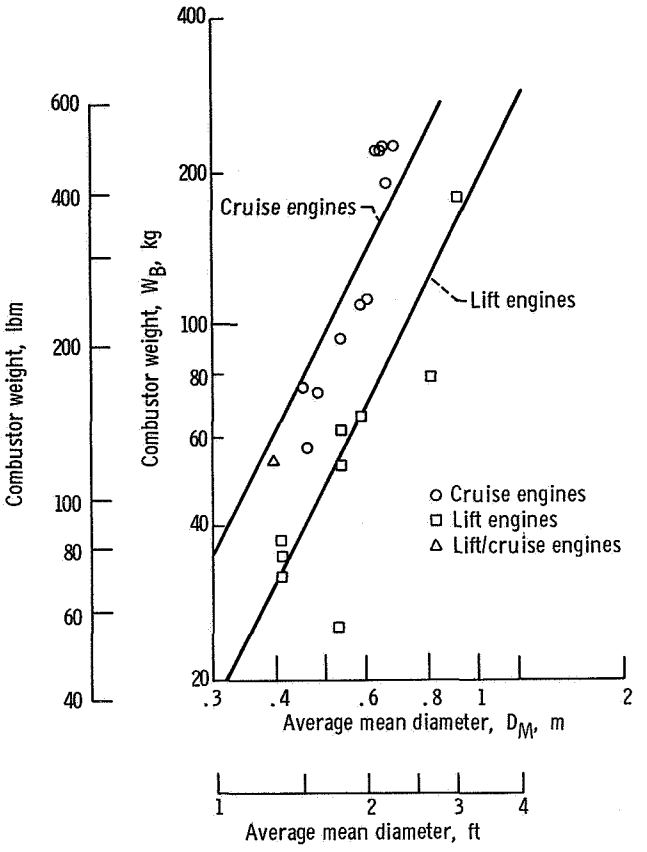

Figure 15. - Combustor weight correlation.

and lift engine combustors was found, with

$$K_B = 195 \qquad (40 \text{ for } \overline{D}_M \text{ in ft, } W_B \text{ in lbm}) \quad \text{for lift engines}$$

$$K_B = 390 \qquad (80 \text{ for } \overline{D}_M \text{ in ft, } W_B \text{ in lbm}) \quad \text{for cruise engines}$$

The more extensive use of titanium in the casing may account for much of this difference. Also, the lift engine combustors were, in general, more compact and designed for lower pressures.

Although the effect of length and pressure on combustor weight could not be established from the data, equation (26) may be altered to reflect the combustor compactness. This may be done by including a length to height ratio term:

$$W_B = K_B \bar{D}_M^2 \left[\frac{\frac{L_B}{H}}{\left(\frac{L_B}{H}\right)_{Ref}} \right]^a \tag{27}$$

where the exponent a was assumed to have a value of 0.5, and

$$\left(\frac{L_B}{H}\right)_{Ref} = 1.6 \quad \text{for lift engines}$$

$$\left(\frac{L_B}{H}\right)_{Ref} = 3.2 \quad \text{for cruise engines}$$

TURBINE

Turbine data were obtained from engines with one, two, and three spools with various flowpath designs. A diagram of a turbine stage model and notation is shown in figure 16.

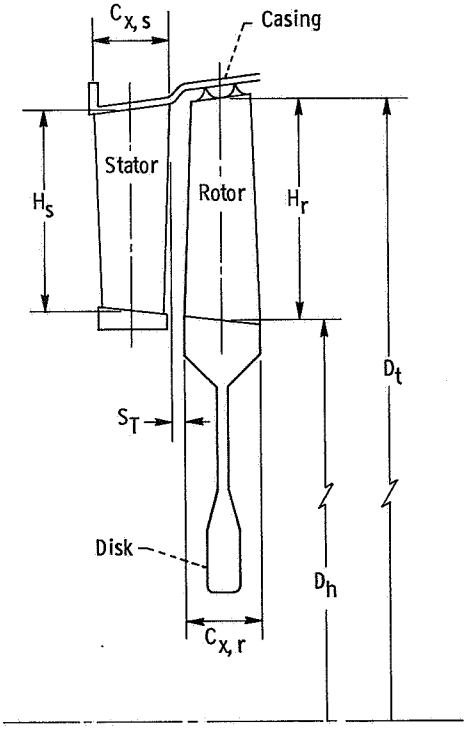

Figure 16. - Turbine stage diagram.

Length

Because the turbine generally consists of a relatively few number of stages compared to compressors, the overall length L_T was estimated by adding the axial lengths of the individual blade rows and clearances between blade rows. In terms of the average (all stages) axial chord length $\overline{C}_x$ and the average clearance $\overline{S}_T$, the turbine length (excluding possible exit straightening vanes) is

$$L_T = N_T(\overline{C_{x,r}} + \overline{C_{x,s}}) + (2N_T - 1)\overline{S}_T \tag{28}$$

In order to estimate the axial chord of the rotor and stator blades, individual blade axial aspect ratios AR_x were correlated with blade row hub-tip diameter ratios for rotor and stator as shown in figures 17 and 18. As can be seen in the figures the data varied widely, especially for the stator. However, when data from any particular turbine (denoted by like symbols in the figures) were examined, more consistent trends with hub-tip diameter ratio were evident. The turbine blade axial aspect ratio was taken to vary with hub-tip diameter ratio as

$$AR_x = A + B\frac{D_h}{D_t} \tag{29}$$

Values found for the factors A and B are given in table III for the various engine types and spools. The trends given by equation (29) may be considered realistic while the absolute values are representative only in that they are within the extremes of the available data.

The average aspect ratios $\overline{AR}_x$ for rotor and stator are determined from equation (29) with the use of the average hub-tip diameter ratio $\overline{D_h/D_t}$. The average axial blade chord $\overline{C}_x$ for rotor and stator rows for use in equation (28) is then found by

$$\overline{C}_x = \frac{\overline{D}_t - \overline{D}_h}{2\overline{AR}_x} \tag{30}$$

where $\overline{D}_t$ and $\overline{D}_h$ may be determined, for example, from engine cycle calculations.

The average clearance between blade rows $\overline{S}_T$ was assumed to be proportional to the average rotor axial chord:

$$\overline{S}_T = a_T\overline{C_{x,r}} \tag{31}$$

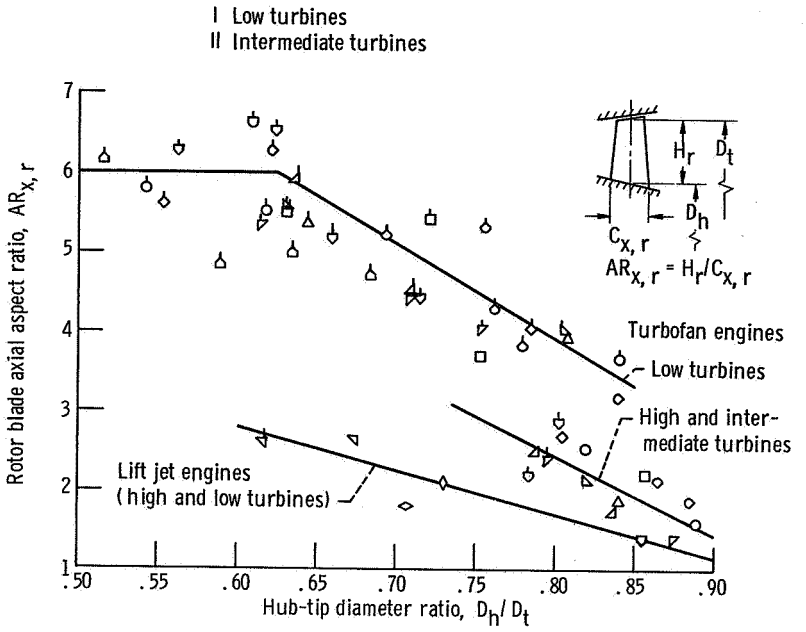

Figure 17. - Turbine rotor aspect ratio.

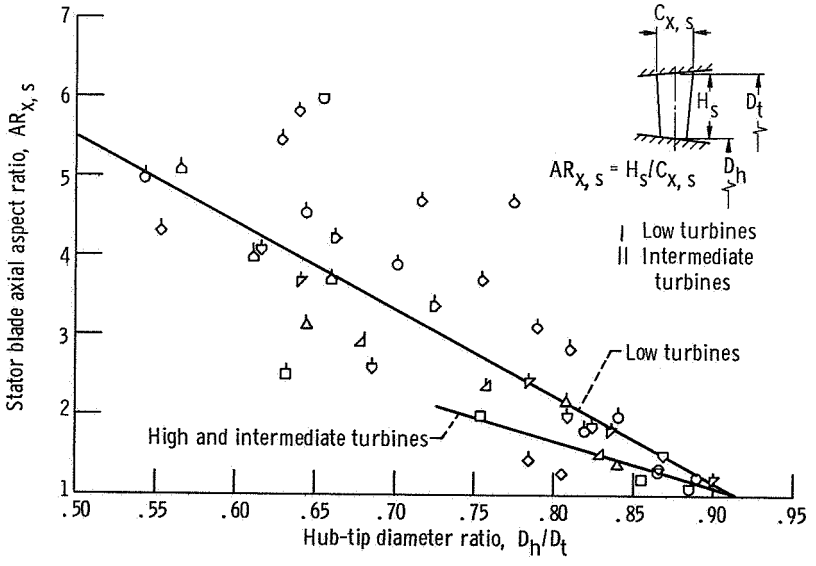

Figure 18. - Turbine stator aspect ratio.

TABLE III. - CONSTANTS IN TURBINE BLADE

ASPECT RATIO EQUATION (EQ. (29))

(a) Turbine rotor

	A	B
Turbofan engines (cruise and lift):		
High and intermediate pressure spool	10.45	-10.0
Low pressure spool[a]	13.36	-11.78
Lift jet engines:		
High and low pressure spools	6.1	-5.5

(b) Turbine stator

	A	B
All engine types:		
High and intermediate pressure spool	6.45	-5.97
Low pressure spool	10.95	-10.9

[a]In this case, AR_x is limited to a maximum value of 6.

For the turbine data investigated, the proportionality constant a_T was found to vary from 0.2 to 1.0. Since length will be critical for VTOL powerplants, a value of 0.3 or 0.4 can be considered representative for high and low pressure turbines.

The number of turbine stages N_T must be specified in order to complete the evaluation of equation (28). The N_T may be a parametric variable in cycle studies or it may be dictated by the work, speed, and efficiency requirements for a given application. A systematic procedure for determining N_T was not developed here.

Weight

The turbine weight includes the rotor disk and blades, stator blades, seals, and casing. From analysis of a simplified multistage turbine model, it was found that the weight equation should be of the form

$$W_T = K_T(\bar{D}_M)^{3-a}N_T(\bar{U}_M)^{2-b} \tag{32}$$

where

$$\overline{D}_M = \frac{1}{2}(D_{M,1} + D_{M,2})$$

and

$$0 < a < 1, \qquad 0 < b < 2$$

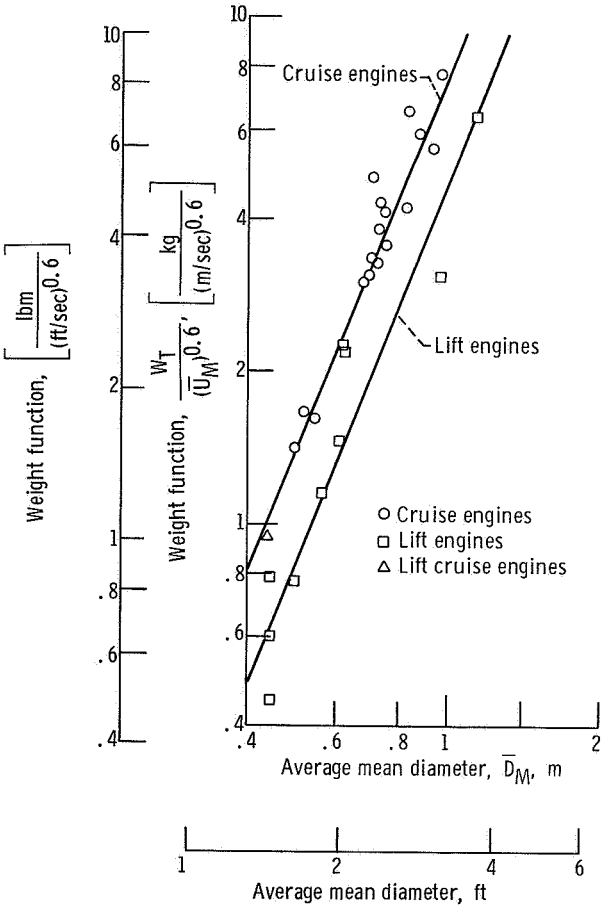

Figure 19. - Turbine weight correlation.

Correlation of turbine weight data with equation (32) gave

$$W_T = K_T(\overline{D}_M)^{2.5}N_T(\overline{U}_M)^{0.6} \tag{33}$$

The correlation is shown in figure 19. As with the compressor and combustor, lift engine turbines were found to be lighter than cruise engine turbines. In equation (33),

$K_T = 4.7$ (0.26 for $\overline{D}_M$ in ft, $\overline{U}_M$ in ft/sec) for lift engines

$K_T = 7.9$ (0.44 for $\overline{D}_M$ in ft, $\overline{U}_M$ in ft/sec) for cruise engines

The use of lightweight materials, such as titanium rotor disks, as well as the reduced design life for lift engines seemed to account for this difference in weight.

CONTROLS AND ACCESSORIES WEIGHT

The components considered in this group include the fuel, control, oil, and starting systems. Not included are airplane power takeoffs or variable geometry mechanisms for inlets and exhaust nozzles. The relations developed for this weight group were obtained from data for lift engines only.

The available lift engine data were correlated with thrust F and fuel flow $\dot{w}_f$. It was assumed that thrust is a sizing parameter for the oil and starting systems, while fuel flow is a sizing parameter for the fuel and controls systems. An equation expressing control and accessories weight was found to be

$$W_A = K_A\left[F + a_A\dot{w}_f\right]$$

or, in terms of thrust and specific fuel consumption SFC,

$$W_A = K_A F\left[1 + a_A(SFC)\right] \tag{34}$$

where $K_A = 0.0002$, and $a_A = 13.2$ ($K_A = 0.002$ and $a_A = 1.35$ for F in lb and SFC in lbm/(lb-hr)).

The lift engine data are compared to equation (34) in figure 20. Considerable variability can be noted in the data. However, since the controls and accessories generally contribute only a small percentage of the total weight of a VTOL powerplant, the error involved may not be significant.

Equation (34) can be applied to lift-system exhaust gas generators by calculating thrust and SFC assuming the exhaust gas is expanded through a nozzle to ambient conditions. Similarly, the thrust and SFC for a lift-system air generator can also be found by assuming the delivered air as well as the exhaust gas are expanded through a nozzle to ambient conditions.

The design requirements for cruise engine control and accessories are significantly different and analogous relations could not be found. Conventional cruise engine control

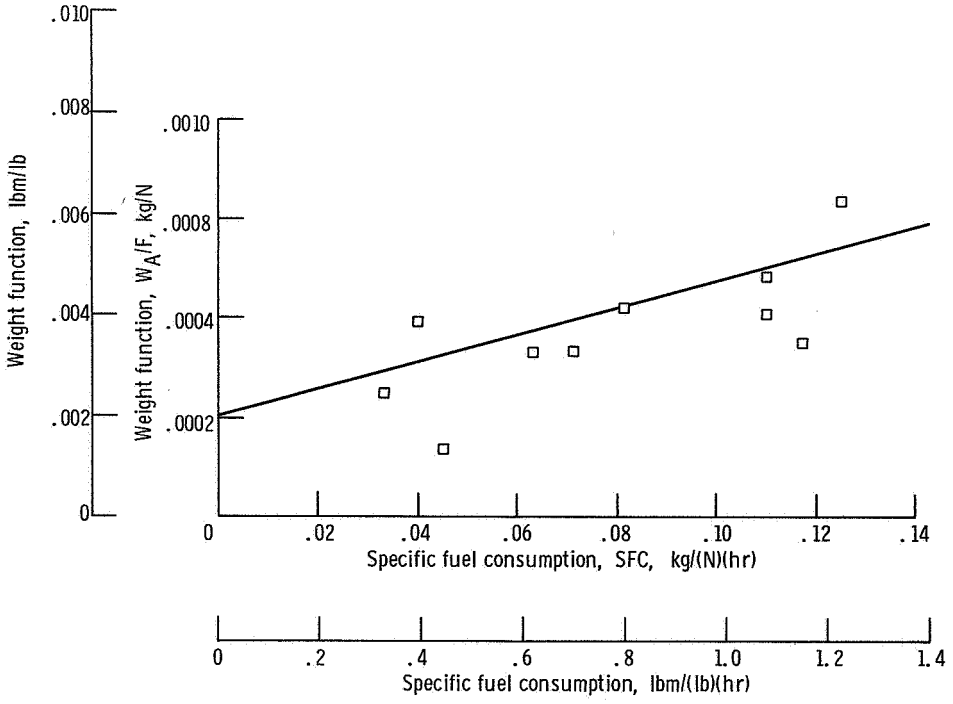

Figure 20. - Lift engine control and accessory weight correlation.

and accessories are generally driven by mechanical drive trains rather than bleed air systems often found in lift engines. Cruise engines provide power for airplane accessories as well. Also, cruise engine controls must operate over a wide range of aircraft speed and altitude and often operate variable inlets and exhaust nozzles. As a result, cruise engine control and accessory weight was found to vary between 9 and 30 percent of the total engine weight compared to a range of from 2 to 10 percent for lift engines.

STRUCTURE WEIGHT

Some additional parts, mainly structural members, were not included in the correlations of the component weights. These parts include the engine mounts, bearings, bearing supports, shafts, inner wall of fan duct (for turbofan engines) and transition sections. The weight of these parts was assumed to vary with the sum of the engine component weights because their design requirements will be dependent on the engine components. Thus, the expression for structure weight was taken as

$$W_S = K_S\left[\sum W_{components}\right] \tag{35}$$

Equation (35) was assumed to apply to turbojet, gas generator, and compressed air

generator powerplants. In the case of a turbofan engine, the fan duct and acoustic lining were assumed to be independent of the structural weight and were, therefore, not included in $\left[\Sigma W_{components}\right]$.

The structure weight correlation coefficient K_S was evaluated for the available engine data:

$$K_S = \frac{\left(W_{total}\right)_{actual}}{\left[\Sigma W_{components}\right]_{calculated}} - 1 \tag{36}$$

where the actual total engine weight $\left(W_{total}\right)_{actual}$ and the sum of the calculated component weights do not include the fan duct weight or acoustic treatment weight for turbofan engines. For cruise engine data, the control and accessory weight was also excluded.

Values of K_S found for the data are shown plotted against $\left(W_{total}\right)_{actual}$ in figure 21. A value of 0.10 was taken to be representative for lift engines. A corresponding value of 0.18 was taken for cruise engines. But since the control and accessory weight was excluded in the cruise engine data, this value is somewhat artificial. It does, however, indicate the relative difference to be expected between cruise engine and lift engine structure weight.

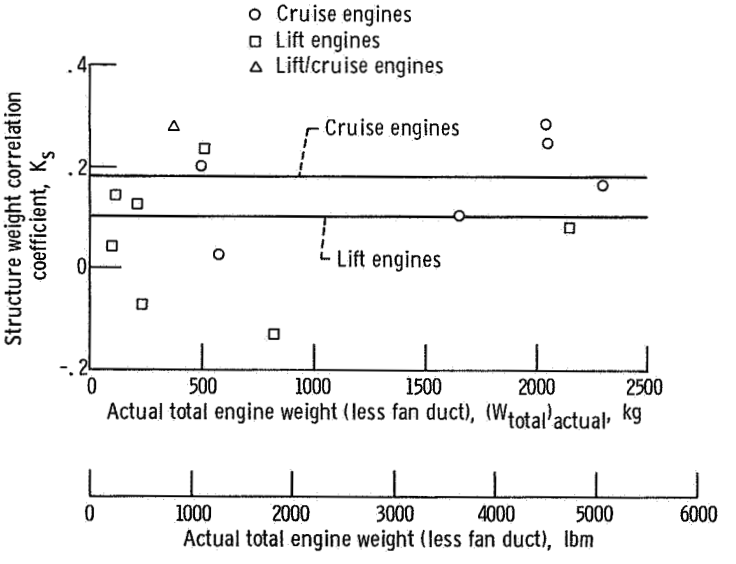

Figure 21. - Structure weight correlation.

TOTAL ENGINE WEIGHT

A total powerplant weight can be determined by using the equations developed herein to sum the estimated component weights including the structure weight. For example, the total weight of a lift turbofan engine may be expressed as

$$W_{total} = W_F + (W_D + W_L) + W_C + \left(W_T\right)_{high} + \left(W_T\right)_{low} + W_A + W_S$$

In order to evaluate the accuracy of the estimated weight summation, total weights of several representative lift and cruise engines (also used in the component weight correlations) were calculated and compared to the reported values. Because of the limited information that was available on any single engine, the component weight equations used for the calculations were those where all terms were established from the data (i. e., eqs. (5), (19), and (26)). Values for the geometric and thermodynamic variables in the weight estimating equations were obtained from the actual engine data. As was done in the structure weight correlation, the controls and accessories weight was excluded for the cruise engines.

Comparisons were made for all the available complete sets of lift engine data and some representative cruise engine data as shown in figure 22. Of the 14 engines, four

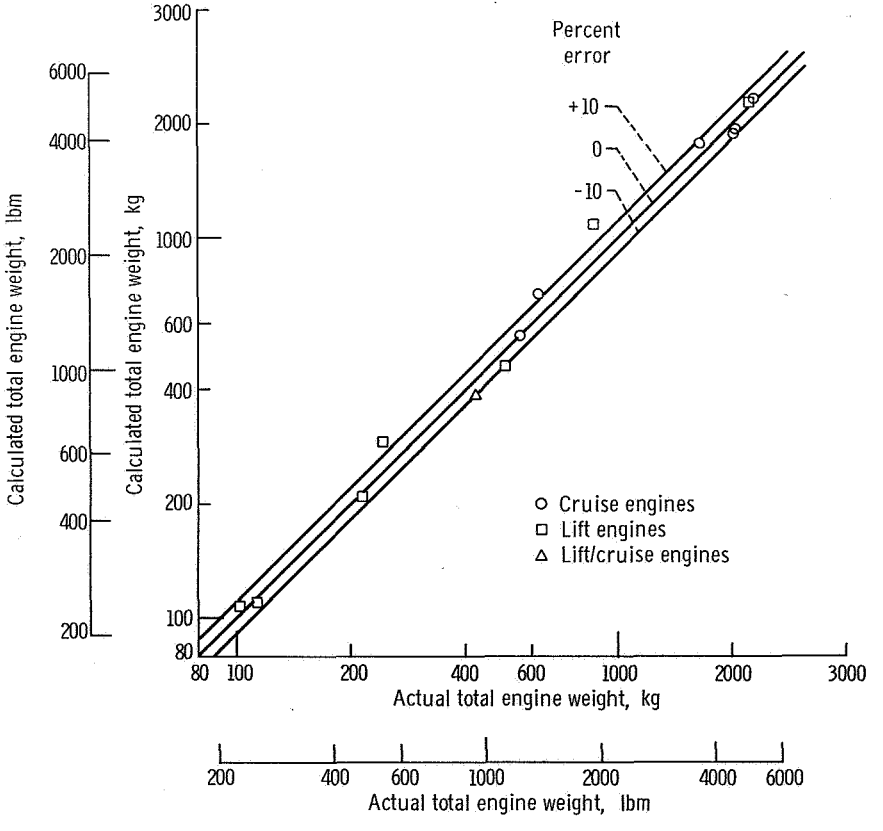

Figure 22. - Total engine weight comparison.

in the demonstrator stage of development and ten were in the preliminary design stage of development. Although it might seem desirable to compare only production engine data, this information is nonexistent for lift engines. Further, production engines do not truly represent the technology level that will probably be used in future VTOL powerplants.

Of the 14 engines compared in the figure, the total weights of only two were estimated with an error significantly greater than ±10 percent. Thus, much of the variation found in the component weight correlations was removed in the summing process of estimating the total engine weight. Apparently the cause of the variation in the component weight data was at least partially due to variations in the parts that were included in the actual component weights.

CONCLUDING REMARKS

Expressions for estimating the length and weight of axial flow components of VTOL powerplants, with the exception of remote lift fans, are presented in this report. They were developed primarily for use in parametric analyses of powerplants suitable for VTOL transport aircraft. These expressions were developed from correlated lift and cruise engine data with the aid of simplified component models. Because of differences in reported details as well as in design approaches and requirements, considerable variability was noted in the component data. However, when comparisons were made between estimated and actual total engine weight for several representative engines, agreement to within ±10 percent was found for nearly all cases considered.

From specified cycle conditions and component arrangements, the reported equations will give estimates of component as well as overall powerplant weight and length. From these estimates, preliminary relative comparisons of alternative powerplants and component arrangements may be made. Also, the effect of changes in cycle parameters on powerplant weight and length characteristics may be determined.

The equations are believed to be most applicable for relative comparisons rather than absolute predictions or evaluations of final mechanical designs. Care should be taken in using the equations as there are limits on the values the variables may assume for the equations to be applicable. The trends given by the equations may not be valid when applied outside the range of the data used in the correlations. Unusual combinations of variable values may also give false trends.

The estimated weights and lengths should be regarded as reference values because the many design considerations involved in any particular powerplant application are not specifically accounted for in the estimating equations. These considerations include duty cycle and use (i. e., design life, maintainability, reliability, military or commercial, cost, and materials). Furthermore, if long-range time periods are involved,

technology level will be another important consideration. These design considerations, however, may be reflected in the estimating equations through appropriate changes in the proportionality constants.

Because the lift engine data included many engines for military applications, it is believed that the final weight of commercial VTOL system powerplant may be somewhat greater than the weights estimated by the lift weight equations. The cruise weight equations, on the other hand, will tend to give estimates that are conservative. Thus, the powerplant characteristics determined by the cruise and lift relations may be considered as upper and possibly lower limits, representing respectively near-term conservative designs and future advanced designs.

Lewis Research Center,
National Aeronautics and Space Administration,
Cleveland, Ohio, August 5, 1971,
721-03.

APPENDIX - SYMBOLS

A	area, m^2 (ft^2)
AR	aspect ratio
a	exponent, coefficient
b	exponent, coefficient
C	blade chord, m (ft)
c	exponent
D	diameter, m (ft)
d	exponent
F	thrust, N (lb)
H	height, m (ft)
K	proportionality constant
L	axial length, m (ft)
N	number of stages, rings
P	total pressure, N/m^2 (lb/ft^2)
R	gas constant, J/kg-K (ft-lb/(lbm-^oR))
S	axial spacing or clearance, m (ft)
SFC	specific fuel consumption, $(kg)_{fuel}/(N)_{thrust}$-(hr) (lbm/(lb-hr))
T	total temperature, K (^oR)
t	thickness, m (ft)
U	blade velocity, m/sec (ft/sec)
V	velocity, m/sec (ft/sec)
W	weight, kg (lbm)
$\dot{w}_a$	air flow, kg/sec (lbm/sec)
$\dot{w}_f$	fuel flow, kg/hr (lbm/hr)
θ	corrected temperature, $\sqrt{T/288}$ ($\sqrt{T(in\ ^oR)/519}$)
ρ	density, kg/m^3 (lbm/ft^3)
σ	solidity

Subscripts:

A	controls and accessories
a	air
B	burner
C	compressor
CMD	constant mean diameter
D	fan duct
F	fan
f	fuel
h	hub
L	acoustic lining
M	mean
m	mass
R	splitter ring
Ref	reference
r	rotor
S	stage, structure
s	stator
T	turbine
t	tip
VMD	varying mean diameter
w	wall
x	axial
1	inlet
2	outlet

Superscript:

$\bar{}$	average

REFERENCES

1. Lieblein, S.: A Review of Lift Fan Propulsion Systems for Civil VTOL Transports. Paper 70-670, AIAA, June 1970.
2. Anon.: Study on the Feasibility of V/STOL Concepts for Short Haul Transport Aircraft. NASA CR-902, 1967.
3. Marsh, K. R.: Study on the Feasibility of V/STOL Concepts for Short-Haul Transport Aircraft. NASA CR-670, 1967.
4. Fry, Bernard L.; and Zabinsky, Joseph M.: Feasibility of V/STOL Concepts for Short-Haul Transport Aircraft. NASA CR-743, 1967.
5. Gerend, Robert P.; and Roundhill, John P.: Correlation of Gas Turbine Engine Weights and Dimensions. Paper 70-669, AIAA, June 1970.
6. Stevens, E. C.: Engine Weight and Size Estimating Techniques. Rep. SEG-TR-66-36, Allison Div., General Motors Corp., Aug. 1966.
7. Merriman, J. E.: Turbofan Engine Weight (TEW I). Rep. DAC-67265, Douglas Aircraft Co., Inc., Apr. 1969.
8. Anon.: Progress of NASA Research Relating to Noise Alleviation of Large Subsonic Jet Aircraft. NASA SP-189, 1968.

NASA-Langley, 1971 —— 28 E-6191